

INFLUENCE OF FIBER UNDULATION ON THE MECHANICAL PROPERTIES OF FIBER REINFORCED PLASTICS

B. Neitzel, C. Fiebig, M. Koch
Department of Plastics Technology
Technische Universität Ilmenau, Germany

ABSTRACT

The classical lamination theory is widely used for the calculation of the mechanical properties of reinforced plastics and stress distribution inside laminates. The resulting Young's moduli along the fiber direction are close to the achievable properties of unidirectional reinforced laminates [1]. However in most applications woven fabrics are used that lower the stiffness of the composites [2]. The influence of undulation and waviness of the fibers on the mechanical properties is yet to be explicitly specified. This article deals with the description of fiber undulation as well as the coherence between the geometry of fabrics and the achievable laminate properties. In order to get improved estimations for the Young's modulus, a new, easily applicable method is introduced to consider the undulation of fibers in the calculation process of the classical lamination theory (CLT). The results show that the given method leads to diminishing the error of the ordinary process.

1. INTRODUCTION

Existing models that describe fiber undulation are the mosaic model, as well as the crimp model, both of which were developed and analyzed by Ishikawa et al. [4].

The mosaic model simplifies the crossing weave and weft structure of the fabric to double stacked cells that each contain fibers solely in 0° or 90° angle to the laminate coordinates (Fig. 1.1).

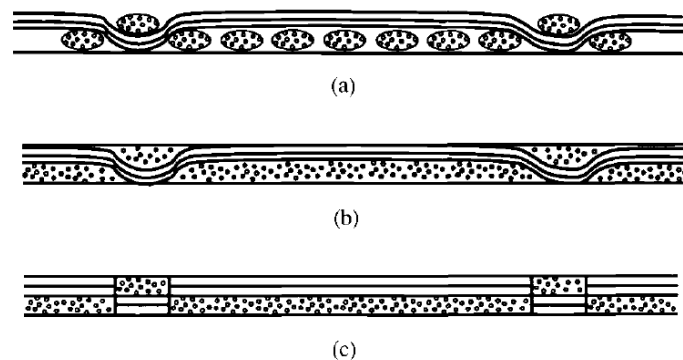


Fig. 1.1. Idealization of the mosaic model. (a) Cross-sectional view of a fabric before impregnation; (b) woven fabric composite; (c) idealization of the mosaic model (After Ishikawa and Chou) [4]

The connection between normalized forces \hat{n} , normalized torques \hat{m} , strains ε , γ and curvatures κ in a laminate is described by the so called ABD-matrix. With $[A]$ being the in-plane stretching stiffness matrix, bending stiffness matrix $[D]$ and bending-stretching coupling stiffness matrix $[B]$. Referred to the mid-plane, the equation (1) is as follows:

$$\begin{Bmatrix} \hat{n}_x \\ \hat{n}_y \\ \hat{n}_{xy} \\ \hat{m}_x \\ \hat{m}_y \\ \hat{m}_{xy} \end{Bmatrix} = \begin{bmatrix} A_{11} & A_{12} & A_{16} & B_{11} & B_{12} & B_{16} \\ A_{12} & A_{22} & A_{26} & B_{12} & B_{22} & B_{26} \\ A_{16} & A_{26} & A_{66} & B_{16} & B_{26} & B_{66} \\ B_{11} & B_{12} & B_{16} & D_{11} & D_{12} & D_{16} \\ B_{12} & B_{22} & B_{26} & D_{12} & D_{22} & D_{26} \\ B_{16} & B_{26} & B_{66} & D_{16} & D_{26} & D_{66} \end{bmatrix} * \begin{Bmatrix} \varepsilon_x \\ \varepsilon_y \\ \gamma_z \\ \kappa_x \\ \kappa_y \\ \kappa_{xy} \end{Bmatrix}_0 \quad (1)$$

By alternating the stiffness constants matrices [A], [B] and [D], the mosaic model can be integrated into the classical lamination theory when the dimensions of the fabric and composite are known.

There are two possible approaches to applying this theory. Either the idealized fiber regions are regarded as parallel or serial working springs (Fig. 1.2).

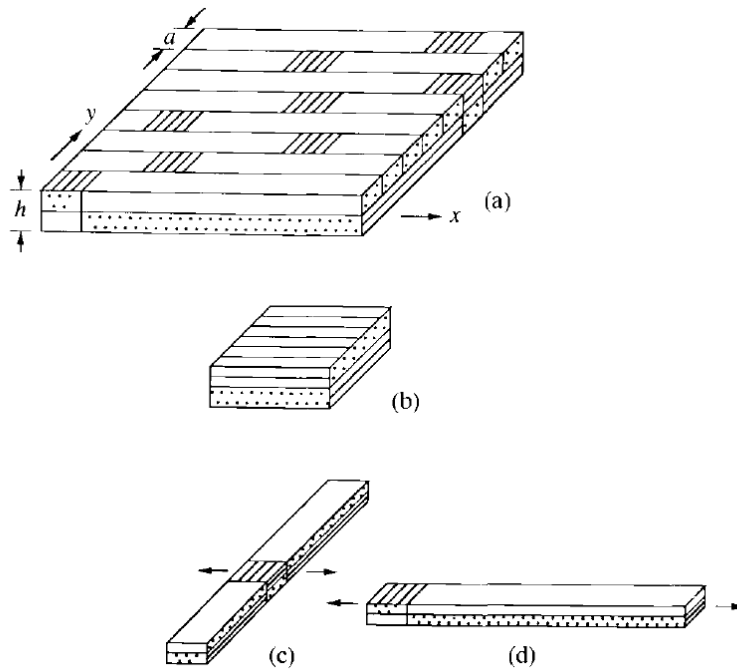


Fig. 1.2. The mosaic model. Repeating region in an eight-harness satin composite; (b) a basic cross-ply laminate; (c) parallel model; (d) series model (After Ishikawa and Chou) [4]

Chou [3] shows the comprehensible solution. Resolving the equations for both possible ways leads to two different results. The use of the parallel model leads to an upper bound for the calculation of the stiffness matrices [A], [B], [D] and a lower bound for the inverted compliance matrices [A'], [B'], [D']. Whereas using the series model leads to a lower bound of [A], [B], [D] and an upper bound of [A'], [B'], [D']. It is not defined which approach should be used, and the obtained results are two extreme values. Furthermore fiber continuity is ignored in this model [5]. In order to consider fiber continuity, another model for fiber undulation, the crimp model, was developed by Ishikawa and Chou [4].

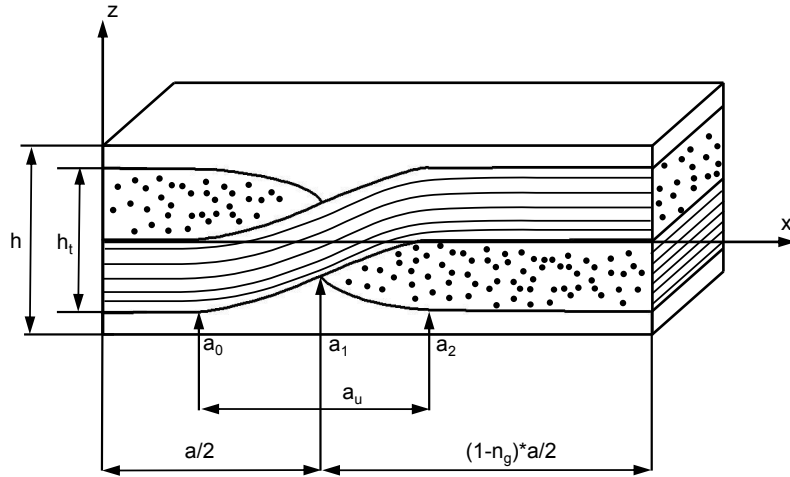


Fig. 1.3. Crimp model (After Ishikawa and Chou) [4]

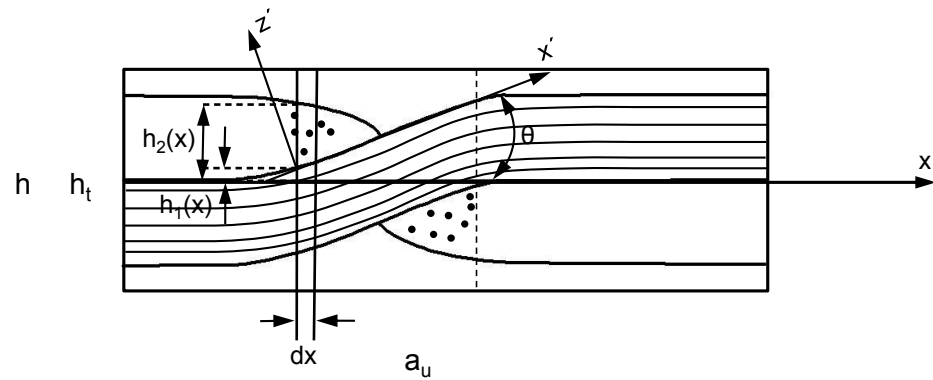


Fig. 1.4. Crimp model detailed cross-section of the fabric (After Ishikawa and Chou) [4]

The crimp model delivers a detailed description of the fiber geometry. It is based on the assumption, that depending on the position inside the composite, different fiber volume fractions are locally present. For each segment a_i the ratio of weave, weft yarn and resin is determined. The properties of every infinitesimal position are integrated to make up the stiffness constants matrix of the ply. Again Chou [4] presents a comprehensible solution for the $[A]$, $[B]$ and $[D]$ matrices. However due to the complexity of the integrands, numeric methods were used in the calculation process [4].

Finally, a bridging model was developed, that is a mixture of the mosaic- and the crimp-model, specifically designed for satin weave [4, 2]. Since it is not applicable for every type of weave, it is of no further interest in the search of a universally usable solution.

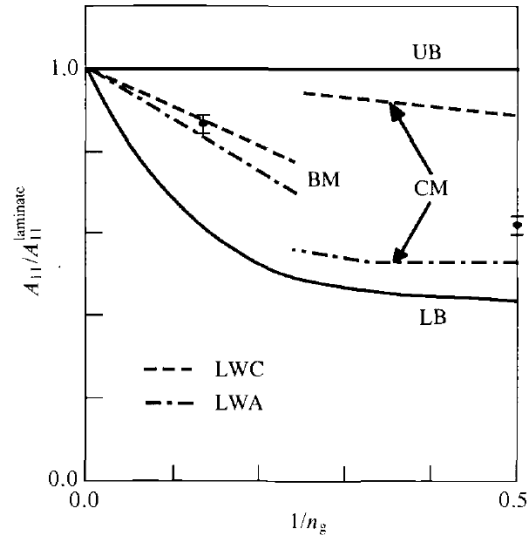


Fig. 1.5. Relationships between non-dimensionalized in-plane stiffness and $1/n_g$ (type of weave) including experimental results [6] with upper- and lower bound of the mosaic model (UB, LB), crimp model (CM) and bridging model (BM)

Mechanical experiments show that the bridging model gives reasonable predictions for the Young's modulus of an eight harness satin weave (Fig. 1.5). The mosaic model as well as the crimp model are able to enclose the mechanical results between their upper and lower bounds. However the possibilities of narrowing down the experimental results into two boundaries are limited. [7]

In this paper another approach to adjust the calculation in order to include fiber undulation is chosen. The developed model is based on the anisotropy of laminates. Due to fiber undulation, the yarns are not aligned ideally in one horizontal direction, but in a vertical angle.

The anisotropy of planar laminates is already included in the classical lamination theory, by the transformation of the local fiber coordinate system to global x-y coordinates. By depicting a single fiber in a dice of a matrix, it becomes obvious, that an angle in vertical direction affects the material properties the same way a horizontal angle does.

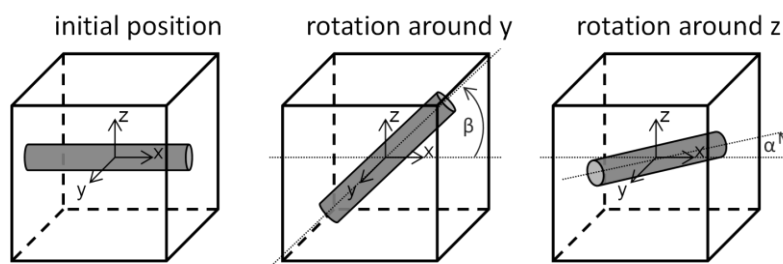


Fig. 1.6. Rotation of a single fiber in a matrix dice

To determine the undulation angle β , there are two possible ways. Producing a laminate and measuring the angle directly under a microscope, or calculating it by using the data of the desired fabric before lamination.

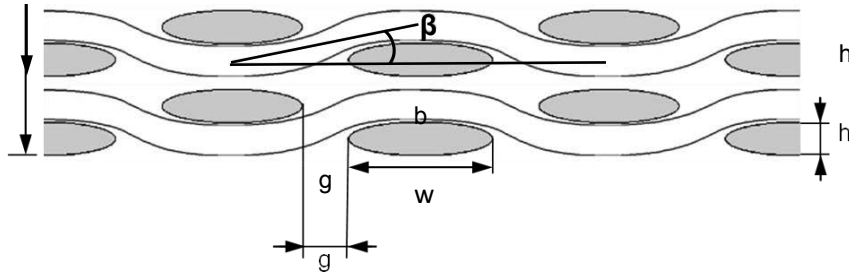


Fig. 1.7. Geometry of a cross section of plain weave fabric

To calculate the angle, the gap g between the yarns, the width w and height h of the yarn, as well as the thickness t of a single layer need to be known.

The thickness can be calculated when the desired or process determined fiber volume fraction φ is known, as well as the grammage of the fabric m_g and the density of the fiber material ρ_f .

$$t = m_g \cdot \frac{1}{\rho_f \cdot \varphi} \quad (2)$$

Each single ply contains two stacked fiber strains, therefore the height of the yarn is:

$$h = \frac{t}{2} \quad (3)$$

Gap and width cannot be calculated and have to be measured on the dry fabric. With all parameters given, the average undulation angle follows as:

$$\beta = \arctan\left(\frac{2}{n_F + 1} \cdot \frac{h}{g + w}\right) \quad (4)$$

Where n_F is the number of weft yarns the warp yarn crosses, before the yarn changes its position inside the fabric from the upper to the lower layer.

In order to apply the undulation angle β , the proceedings of the classical lamination theory has to be extended by one step after the stiffness matrix $[Q]$ of the unidirectional material mix is arranged. The partial transformation regarding the undulation angle takes place as a second step. It is assumed, that the Q_{11} stiffness constant is exclusively affected by undulation.

$$[Q_{fabric}] = \begin{bmatrix} Q_{11} \cdot \cos^4(\beta) + 2(Q_{12} + 2Q_{66}) \cdot \sin^2(\beta) + Q_{22} \cdot \sin^4(\beta) & Q_{12} & 0 \\ Q_{12} & Q_{22} & 0 \\ 0 & 0 & Q_{66} \end{bmatrix} \quad (5)$$

The stiffness matrix $[Q_{fabric}]$ is now the basis for the ordinary steps of the classical lamination theory.

2. EXPERIMENTAL

The test specimen consist of the fabric types according to Table 2.1:

Table 2.1 Fabric types used for specimen preparation

	Unit	Plain weave	Twill weave	Unidirectional
Manufacturer	[/]	PD-Interglas	PD-Interglas	HP-Textiles
Fabric designation	[/]	92130	92140	UD-fabric
Grammage	[g/m ²]	390	390	400

EPIKOTE RIMR 135 was used as epoxy resin matrix together with EPIKURE RIMH 134 curing agent. Laminates with a stack up of ten layers were produced. The manufacturing temperature was 23°C, curing took place at 23°C for 24 hours followed by 60°C for another 15 hours.

Due to unidirectional fabric only having 10% weft yarns for handling reasons, weave induced fiber undulation can be neglected.

Specimen according to DIN EN ISO 527-4 Type 3 were cut. The fiber undulation at the cross section was examined under a Zeiss Stemi 200-C stereo microscope and interpreted with the aid of the Zeiss AxioVision software. Furthermore dry samples of the used fabric were gauged alike in order to obtain the values needed for calculating the undulation angle.

Additional specimen were produced in an 90° angle with radii R of 5 mm and 10 mm (Fig. 2.1), which are used to analyze possible changes of the undulation angle in curved laminates.

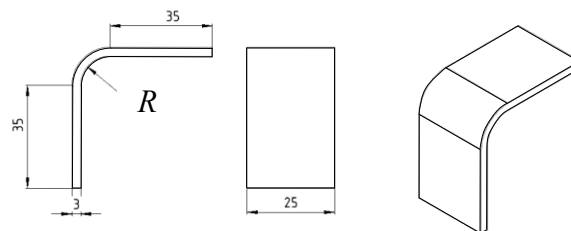


Fig. 2.1. Curved specimen

Tests of the Young's modulus were performed in accordance to the DIN-EN-ISO 527-4 on a universal testing machine with clamp-on extensometer.

3. RESULTS AND DISCUSSION

The theoretical undulation angles for plain weave and twill weave were calculated with the aid of measurements of the dry cloth under microscope (Fig. 3.1) and typical fiber volume contents from test laminates:

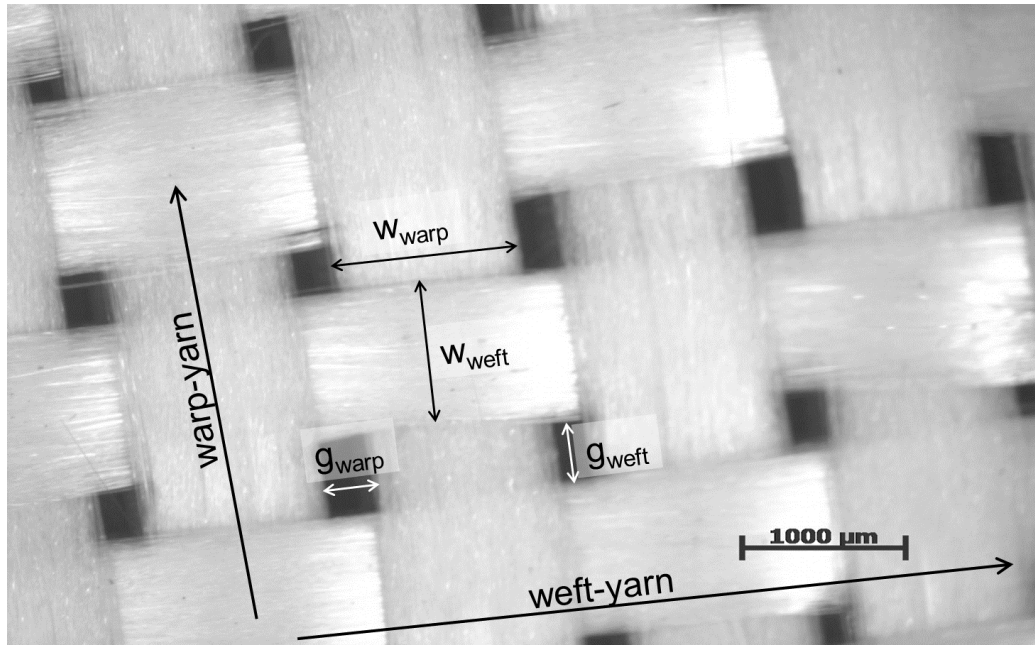


Fig. 3.1 Parameters for fabric measurement

Table 3.1. Fabric measurements and calculated undulation angle

	Unit	Value
Width warp yarn w_{warp}	$[\mu\text{m}]$	1243.49 ± 32.82
Width weft yarn w_{weft}	$[\mu\text{m}]$	1195.90 ± 76.71
Gap warp yarn g_{warp}	$[\mu\text{m}]$	198.25 ± 62.48
Gap weft yarn g_{weft}	$[\mu\text{m}]$	385.70 ± 87.17
Grammage	$[\text{g}/\text{m}^2]$	390
Fiber density ρ_{fiber}	$[\text{g}/\text{cm}^3]$	2.60
Fiber volume content ϕ_{plain}	$[\%]$	50.99
Fiber volume content ϕ_{twill}	$[\%]$	52.53
n_{F} plain weave	$[\]$	1
n_{f} twill weave	$[\]$	2
Undulation angle plain weave β_p	$[\]$	$5.42 \pm 1.1 \cdot 10^{-4}$
Undulation angle twill weave β_t	$[\]$	$3.94 \pm 1.1 \cdot 10^{-4}$

In order to review the possible changes of the angle by manufacturing parameters, a prototype laminate was produced. The test laminate was made in a vacuum infusion process. By cutting the laminate and examining the cross section, the undulation angle can be measured directly. A measurement of 30 samples resulted in an angle β_p of $5.67 \pm 0.35^\circ$, which shows that using the parameters of dry cloth and estimating the fiber volume content delivers reliable results for the prediction of the undulation angle.

Curved specimen were additionally manufactured in a vacuum infusion process with the same process parameters as the flat laminates. There are two effects influencing the deformation of the yarn in curved laminates. By putting the fabric preforms onto a curved tool, its weight causes the yarn which is orthogonal to the curvature to spread along the edge, increasing the yarn width and decreasing the according yarn height. Contrary to this effect, due to compressive forces of the atmospheric pressure during the manufacturing process the yarn gets additionally deformed (Fig. 3.2).

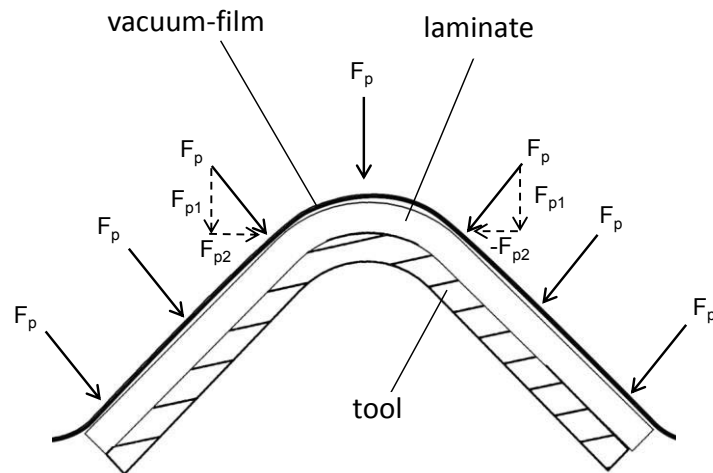


Fig. 3.2. Atmospheric pressure during vacuum infusion

The measurement of the undulation angle showed, that small radii can influence the width of the weft yarn (Fig. 3.3).

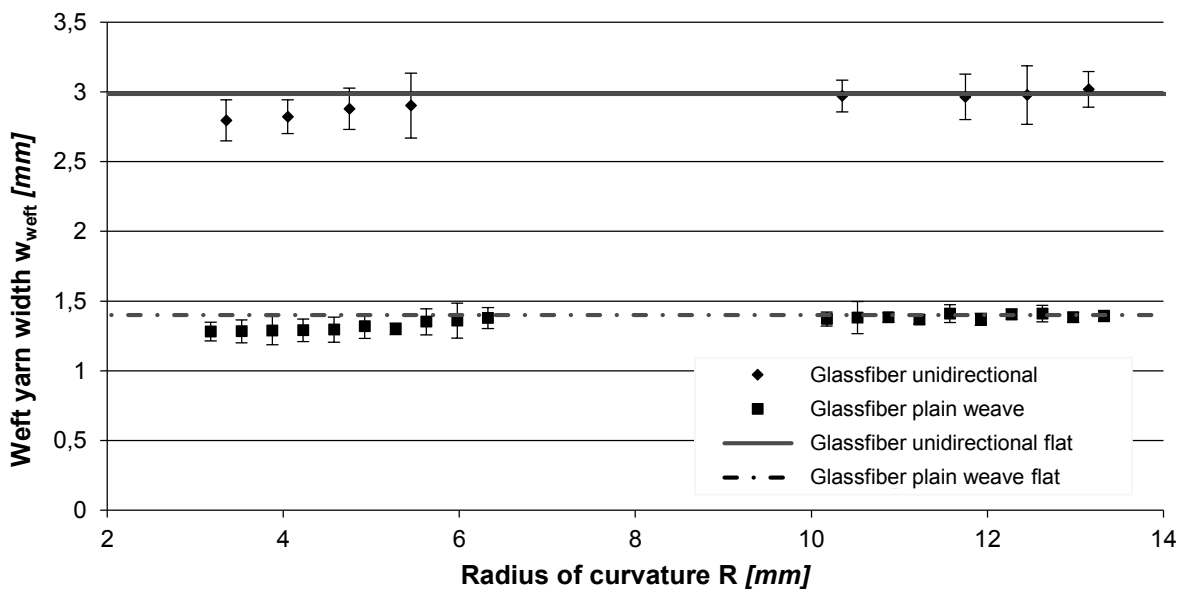


Fig. 3.3 Coherence between radius of curvature and width of the weft yarn

Since the width of the deformed yarn converges towards the flat measurement at larger radii, it becomes obvious that the compressive forces are predominating.

According to Fig. 3.3 at the smallest radius an average deviation in width of 0.19 mm for unidirectional and 0.12 mm for plain weave fabric was measured. This equals a deviation of the undulation angle of 0.39°.

The Young's modulus E_x was calculated using the theoretical undulation angles and the following material properties:

Table 3.2. Material properties

	Unit	Fiber	Resin
Young's modulus E	[GPa]	73.00	3.20
Shear modulus G ₁₂	[GPa]	30.40	1.23

Flat laminates with unidirectional (0°/90°), plain weave and twill weave fabric were manufactured using vacuum infusion with constant parameters. After the curing process, specimen according to DIN EN ISO 527-4 were cut and the Young's modulus was measured. In order to eliminate a systematical error in the universal testing machine, the recorded curves were corrected to fit the values of unidirectional fibers, since the effect of undulation is insignificant in this type of fabric.

Table 3.3. Summary of measured laminate properties

	Unit	Unidirectional (0°/90°)	Plain weave	Twill weave
Fiber volume content φ	[%]	50.50 ± 0.66	58.91 ± 0.95	59.29 ± 0.59
Theoretical Young's modulus E _x (CLT)	[GPa]	22.45	25.96	26.09
Theoretical Young's modulus E _x (undulation)	[GPa]	22.45	23.64	24.79
Experimental Young's modulus E _x	[GPa]	22.45 ± 0.49	21.98 ± 0.72	24.19 ± 0.26

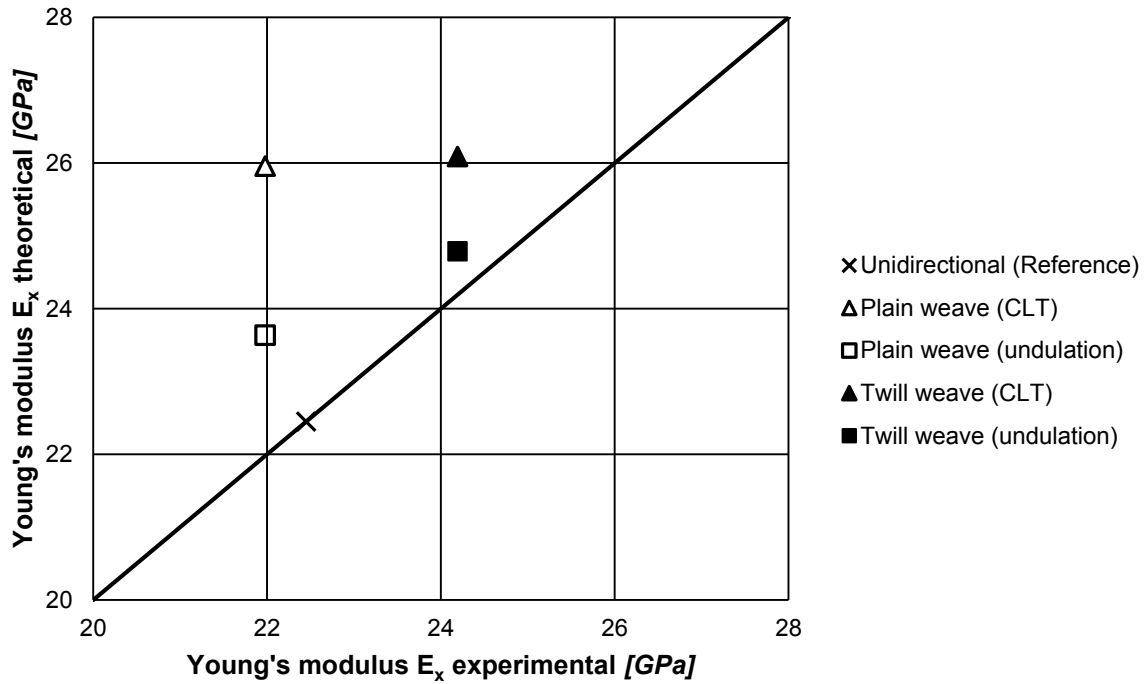


Fig. 3.4. Comparison between theoretical Young's modulus and experimental results

4. CONCLUSIONS

Fiber undulation reduces the stiffness of fiber reinforced composites. Plain weave fabric shows the sharpest decrease in the Young's modulus due to the highest possible amount of fiber crossings, followed by twill weave with crossings at every second yarn. This aspect is taken into account by the use of the undulation angle. While the Young's modulus of the plain weave laminate shows an error of 18.1% and twill weave of 7.8% when calculated by CLT, it is reduced to 7.5% and respectively 2.5% when the undulation angle is considered.

The calculated moduli are always higher than the measured ones. The difference of the measured undulation angle in the laminate compared to the result of the calculation with the aid of the measured geometry of the dry fabric is negligible. Since the yarn width, height and the gap between yarns is constant for every type of fabric, the undulation angle needs to be determined only once and could be given in the according data sheet. Curved specimen with small radii show a deviation of the yarn width due to compressive forces, which result in an error of the calculation of the undulation angle. The effect of yarn compression in curved areas should be further examined for the resin transfer molding process, since different pressure conditions are present. However the impact of the thereby induced differing undulation angle on the mechanical properties should be little in comparison to other effects, like the uneven distribution of fibers and matrix in curved areas that lower the interlaminar shear strength [1]. Applying the undulation angle considers the decrease of stiffness in consequence of the fibers not being aligned parallel to the direction of the load. However further influences of fiber undulation, like the distribution of porosity and matrix cannot be taken into account. Those parameters possibly are the cause of the experimental Young's moduli being lower than the calculated ones. Nevertheless this approach enhances the results of the CLT by adding a single matrix transformation and can be used to exploit lightweight potential at a higher rate.

REFERENCES

- [1] H. Schürmann, „Konstruieren mit Faser-Kunststoff-Verbunden“, Springer, Berlin, 2007.
- [2] T. C. Henry, C. E. Bakis and E. C. Smith, “Determination of Effective Ply-level Properties of Filament Wound Composite Tubes Loaded in Compression”, Journal of Testing and Evaluation, 43, 2015.
- [3] T.-W. Chou, “Microstructural design of fiber composites”, Cambridge University Press, Cambridge, 1992.
- [4] T. Ishikawa and T.-W. Chou, “Stiffness and strength behaviour of woven fabric composites”, Journal of Material Science, 17, 1982.
- [5] A. Miravete, “3-D Textile Reinforcements in Composite Materials”, Woodhead Publishing, Cambridge, 1999.
- [6] T. Ishikawa, M. Matsushima, Y. Hayashi and T.-W. Chou, “Experimental Confirmation of the Theory of Elastic Moduli of Fabric Composites”, Journal of Composite Materials, 19, 1985
- [7] A. Kelly, “Concise Encyclopedia of Composite Materials”, MIT Press, Cambridge, 1989.

CONTACTS

M. Sc. Benedikt Neitzel
Dipl. –Ing. Christian Fiebig

benedikt.neitzel@tu-ilmenau.de
christian.fiebig@tu-ilmenau.de